ACS OMEGA

Open Access

http://pubs.acs.org/journal/acsodf

Article

Characteristic Improvement of a Carrageenan-Based Bionanocomposite Polymer Film Containing Montmorillonite as Food Packaging through the Addition of Silver and Cerium Oxide Nanoparticles

Gita Genecya, Damar R. Adhika,* Widayani Sutrisno, and Triati D. K. Wungu

Cite This: *ACS Omega* 2023, 8, 39194−39202

Read Online

ACCESS | Metrics & More | Article Recommendations

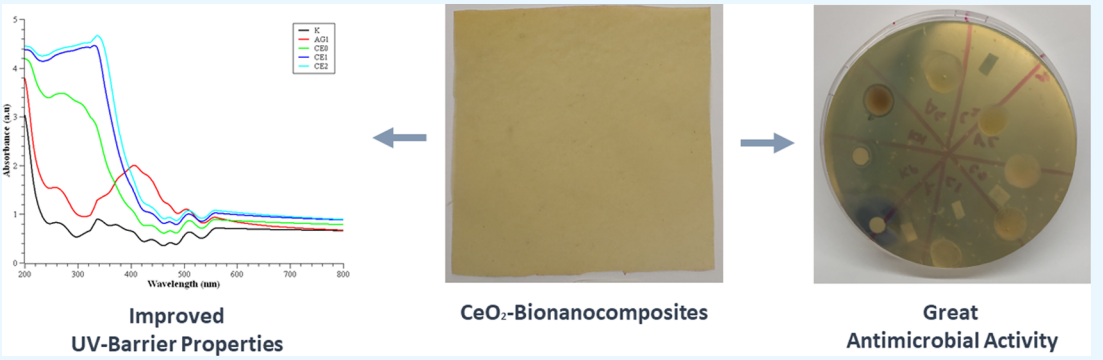

ABSTRACT: Plastic has become an essential ingredient in social life, especially in its function as food packaging. An increase in plastic consumption can have a big impact, especially on environmental issues, because of the plastic waste produced. Substituting petroleum-based plastic with bionanocomposites can be done to reduce the impact of environmental issues caused by plastic waste. The purpose of this study is to produce nanoparticle-incorporated bioplastics, which can be applied as alternative food packaging, especially as petroleum-based plastic substitutes, and as food packaging that has added value in the form of antimicrobial properties. In addition, nanoparticles are also intended to improve the characteristics of bioplastics such as improving mechanical properties and film permeability as well as increasing the barrier properties of bioplastics against ultraviolet rays that can damage packaged food. Bionanocomposites with modified forms were investigated by various characterization such as Fourier transform infrared (FTIR), mechanical property testing of bioplastics as well as analysis of water vapor permeability (WVP), scanning electron microscopy (SEM), thermogravimetric analysis (TGA), differential scanning calorimetry (DSC), UV−visible spectrophotometry (UV−vis), and antimicrobial testing. Visible improvement of mechanical and UV barrier properties was seen in bionanocomposites with the addition of cerium nanoparticles. Furthermore, we have also demonstrated the antibacterial activity properties of nanoparticle-loaded bionanocomposites, which can add value to their use as food packaging. These results indicate that carrageenan-based bionanocomposites have a high potential for positive application in food packaging to ensure food safety and extend the shelf life of packaged foods.

INTRODUCTION

Plastics are popularly used for food packaging due to their low cost, ease of handling, stability, and good mechanical properties.[1−3] Conventional plastics are mostly derived from petrochemical monomers, which are nonbiodegradable and not environmentally friendly.[1,4−6] The food industry is the number one end user of packaging that plays a major role in using plastics, accounting for approximately 40% of the overall plastic usage. In addition, there is a 12% increase in plastic usage as food packaging per year, resulting in a huge negative impact on our environment, such as depletion of soil health, climate change, and reduction in water quality, which affects the health of living organisms.[3,6−8] Therefore, biopolymer films were made and continue to be developed as a measure to address the negative impact of plastics on the environment.[4,9,10]

Received: June 26, 2023
Accepted: September 28, 2023
Published: October 12, 2023

Biopolymers are bioderived monomers obtained by chemical synthesis or directly extracted from biomass materials or industrial waste.[11] Recently, biodegradable and renewable polymers from marine-derived sources have been preferable to other biomass sources due to their abundance, high productivity, and continuous availability.[3,12,13] Carrageenan is one of the marine-derived sources of the polymer known to be extracted from seaweed, specifically class Rhodophyceae of red seaweed.[12,14,15] Carrageenan is anionic linear, containing 15−40% sulfated ester bonds polysaccharides. Carrageenan provides an excellent gelling ability and a high solubility and swelling in water, making it biodegradable, and it has been extensively used in food and packaging.[15−17] However, although biopolymers are environmentally friendly, they have a primary limitation of a shorter lifetime, mainly because of their hydrophilic, poor barrier, and thermomechanical properties. This limitation made carrageenan-based biopolymers less in demand as food packaging since food packaging must have good barrier properties to protect its content against external forces and contamination.[18] Various methods can be carried out to improve the properties of biopolymers, one of which is with nanotechnology approaches like incorporating nanofillers.[4,17] Nanofillers could improve biopolymer properties through better mechanical and barrier properties. Nanofillers also enhance the hydrophobicity and melting temperature of biopolymers. Nanofillers, especially nanoclay, also have been known to have the ability to improve the barrier properties of bionanocomposites. Nanoclay creates a longer diffusion pathway to delay the transfer of molecules, improving barrier properties.[19,20] Montmorillonite (MMT) is a widely used nanoclay in food packaging applications.[21] Shojaee-Aliabadi et al.[14] found that using MMT in a carrageenan film can improve the physical and mechanical properties of the film by increasing the tensile strength value. The addition of 5% MMT can also improve barrier properties by lowering the permeability of the carrageenan biopolymer film.[22] Besides mechanical and barrier properties, food packaging needs to protect and prevent its content from microbial contamination. Antimicrobial nanocomposite packaging systems are particularly effective in gaining these capabilities because of the high surface-to-volume ratio and enhanced surface reactivity of nanosized antimicrobial agents, which are highly useful in preventing microbial contamination for extending shelf life and securing food safety.[23,24] There are several antimicrobial agents, one of which is inorganic such as nanoparticles. Nanoparticles are considered to be incorporated into biopolymers to form antimicrobial packaging systems.[25] Silver nanoparticles (AgNPs) have been known as inorganic antimicrobial agents due to their unique properties and low toxicity.[22,23] A study by Rhim and Wang in 2014[22] reported that nanocomposites incorporated by AgNPs have a great antimicrobial effect against Gram-negative bacteria (*Escherichia coli*). However, AgNPs also have a toxic effect on various fungi, including *Aspergillus*, *Saccharomyces*, and *Candida*.[26] Another inorganic material that has an antimicrobial effect is cerium oxide nanoparticles (CeNPs). CeNPs have an antimicrobial effect on Gram-negative and Gram-positive bacteria.[27,28] So far, CeNPs have been produced and applied to various technologies, but there has yet to be a report on producing a biopolymer-based nanocomposite film using CeNPs.

Carrageenan bioplastics as food packaging have the disadvantage of not having antibacterial and UV barrier properties. The novelty in this research is to study the addition of cerium oxide nanoparticles (CeNPs) to provide antibacterial and UV barrier properties to carrageenan-based bioplastics. Therefore, the main objective of the present study is to prepare a bionanocomposite polymer film reinforced with montmorillonite cerium oxide nanoparticles (CeNPs) as an antimicrobial agent. The properties of a bionanocomposite polymer film containing CeNPs will be compared with those with AgNPs. The synthesized AgNPs, CeNPs, and bionanocomposite polymer film are characterized using SEM, UV−vis, and FTIR. In addition, the properties of the carrageenan-based bionanocomposite films, such as mechanical, water vapor barrier, thermal stability, and antimicrobial properties, were evaluated.

EXPERIMENTAL SECTION

Materials. Food-grade k-carrageenan was obtained from a market in Malaysia. Dextrose, montmorillonite, and gum acacia were obtained from a local market in Indonesia. Glycerol and cerium nitrate hexahydrate ($Ce(NO_3)_3{\cdot}6H_2O$) were obtained from Merck Millipore, Germany. Silver nitrate ($AgNO_3$) was obtained from PT. Antam Tbk, Indonesia.

Synthesis of AgNPs. The synthesis of AgNPs was conducted using the sol−gel method with gum acacia as the reducing agent, which was referred from the study of Dong et al.[29] The process began with the preparation of a gum acacia solution. The gum acacia solution was obtained by heating 1 g of gum acacia in 70 mL of deionized water for 90 min at 60−80 °C. The resulting gum acacia solution was then mixed with 30 mL of a 0.1% silver nitrate solution and stirred for 3 h at 60−80 °C until a dark-colored mixture was obtained. The mixture was then centrifuged at 20,000 rpm for 30 min. The resulting precipitate was washed with deionized water to remove impurities. The AgNP solution as the final product was stored at a temperature of 4 °C.

Synthesis of CeO_2NPs. Cerium oxide nanoparticles or ceria nanoparticles (CeNPs) were synthesized using the method referred from Asati et al. publication with slight modification.[28] In brief, 1 mL of cerium nitrate 1 M was added into 2 mL of a 0.1 M dextrose solution. The mixture was stirred while a 0.3 M sodium hydroxide solution was added until the pH reached 9. This addition of sodium hydroxide caused the mixture to turn bright yellow due to its role as a precursor for forming cerium oxide nanoparticles. The mixture was then stirred at room temperature for 24 h. After stirring, the mixture was centrifuged at 20,000 rpm for 30 min. The resulting precipitate was purified with deionized water (DW) and ethanol to remove impurities. The solution of cerium oxide nanoparticles was then stored at 4 °C.

Film Formation. Bionanocomposite films were prepared by a solution casting method. First, precisely weighed MMT (260 mg, 20 wt % of carrageenan) was dispersed into distilled water (5 mL) and sonicated for 5 min to hydrate clay mineral. Aqueous dispersions of k-carrageenan powder (2%, w/w) were then stirred with no heat for 5 min using a hot-plate magnetic stirrer at 2000 rpm. After the carrageenan powder dissolved, a sonicated MMT dispersion was added to the film-forming mixture. The mixture was continuously stirred and heated for 10 min at 80 °C. During the heating process, glycerol as a plasticizer (3%, v/v) was added to the mixture. Completely solubilized and well-dispersed film-forming solutions were cast evenly onto a Teflon plater (d = 16 cm) and dried at 60 °C for 20 h. Dried composite film samples were peeled off of the plate.

https://doi.org/10.1021/acsomega.3c04575
ACS Omega 2023, 8, 39194−39202

Fabrication of bionanocomposite films loaded with nanoparticles began with the preparation of a nanoparticle solution. The nanoparticle solution is prepared by homogenizing using an ultrasonic homogenizer at a 34% amplitude for 10 min before adding it to the bionanocomposite mixture. Bionanocomposite mixtures containing AgNPs and CeNPs have been prepared using several treatment variations. The sample codes used throughout this paper for each nanoparticle addition variation are given in Table 1. The synthesis steps of bionanocomposite films loaded by nanoparticles were identical to those of carrageenan-based bionanocomposite films. The difference lies in the solvent used, which is in the form of a nanoparticle solution.

Table 1. Nomenclature of Bionanocomposite Samples

sample code	treatment
BC-K	bionanocomposites without the addition of nanoparticles
BC-AG1	bionanocomposites with the addition of 1% AgNP (% wt)
BC-CE0	bionanocomposites with the addition of 0.5% CeNP (% wt)
BC-CE1	bionanocomposites with the addition of 1% CeNP (% wt)
BC-CE2	bionanocomposites with the addition of 1.5% CeNP (% wt)

X-ray Diffraction (XRD) Analysis. The XRD patterns of AgNPs and CeO_2NPs were measured using an X-ray diffractometer (Bruker D8 Advance, X-ray Diffractometer) with Cu-Kα at 40 kV and 40 mA. Powder diffraction patterns were obtained in step scanning mode, $2\theta = 10-90°$ and step of 0.02°. The crystallite size of the nanoparticles was calculated using peak height and width. The results were then analyzed by using the Debye−Scherrer equation.

$$D = \frac{0.9\lambda}{\beta \cos \theta}$$

Determination of Particle Size of Nanoparticles. The dynamic light scattering method was used to measure particle size using a particle size analyzer (Horiba, SZ-100) with water as the dispersion medium. The nanoparticle solution was analyzed at room temperature with a fixed angle of 90°.

Transmission Electron Microscopy (TEM) Analysis. Shape and size nanoparticles were analyzed using a transmission electron microscope (TEM Hitachi HT-7700, Japan). Nanoparticles were dispersed in deionized water via sonication, and a small amount of the solution was dispersed on a copper grid. The samples were then mounted on a holder and transferred to the microscope for observation.

Morphology of Bionanocomposites. The morphology of carrageenan-based nanocomposites was observed by using SEM (scanning electron microscopy, Hitachi SU-3500, Japan) operated at an accelerating voltage (V_{acc}) of 10 kV.

Fourier Transform Infrared (FTIR) Spectrophotometry Analysis. The FTIR spectrum of the nanocomposite film samples was analyzed using the FTIR Bruker with the attenuated total reflectance (ATR) method. Samples were placed on the ray exposing stage, and the spectrum for each sample was recorded between the wavenumber range of 500 and 4000 cm^{-1}.

UV−Vis Spectrophotometry Analysis. The UV−vis spectrum of the nanocomposite film was measured on a spectrophotometer. The transparency of the nanocomposite film was determined using UV−vis spectrophotometry at room temperature and a wavelength range of 200−800 nm. Transparency of the film samples was expressed as the following equation

$$\text{transparency} = \log \%T/b$$

where $\log \%T$ is the log of %transmission and b is the thickness of the film (mm).

Thermal Analysis. Thermal analysis of the nanocomposite film is analyzed using differential calory scanning calorimetry (TA-DSC25) with a range temperature of 30−350 °C. Meanwhile, the thermal stability of the nanocomposite film was tested with thermogravimetric analysis (TGA; USA Model Q50) with a range temperature of 30−600 °C. These thermal analysis processes were conducted at a heating rate of 10 °C/min under a nitrogen flow of 50 cm^3/min.

Water Vapor Permeability (WVP). Water vapor permeability tests were conducted using the ASTM method E96-00 with some modifications. First, the nanocomposite film samples' water vapor transmission rate (WVTR) was determined gravimetrically at 25 °C under 40% RH. Later, the WVP of the film was calculated by using the following equation

$$\text{WVP} = (\text{WVTR} \times L)/\Delta p$$

where WVTR is the water vapor transmission rate ($g/m^2 \cdot s$) through the film, L is the mean of film thickness (m), and Δp is the partial water vapor pressure difference (kPa) across two sides of the film.

Mechanical Properties. Tensile strength (TS), elongation at break (EAB), and elastic modulus (EM) were analyzed according to ASTM D882-02 using a universal testing machine (Dongguan Sinowon Precision Instrument SM-10, Dongguan, China) equipped with a 10 kN load cell. Rectangular strips (3 cm × 4 cm) were cut from the individually prepared film. The initial grip separation was set at 50 mm, preload speed at 50 mm/min, and pulling speed at 100 mm/min. The thickness of all of the bioplastics was measured using a Mitutoyo Thickness Gauge Digital.

Antimicrobial Activity. The agar disk diffusion method was used to evaluate the antimicrobial activity of nanocomposite films with the determination of inhibition zones.[20] *Bacillus cereus* as a Gram-positive bacterium and *E. coli* as a Gram-negative bacterium were used as test organisms. Both bacteria were prepared by diluting pure agar culture with sterile saline (0.85%) until the microbial suspension was inoculated at ca. 108 cfu/mL. Then, each microbial suspension (0.1 mL) was uniformly spread on the NA agar plate. Nanocomposite film samples in the form of a round disk of 5 mm diameter were carefully placed on the surface of the agar medium and subsequently incubated at 37 °C for 24 h. The zone of inhibition was then estimated by measuring the diameter of the bacterial growth inhibition zone around the disk of the film samples.

RESULTS AND DISCUSSION

Characterization of Nanoparticles. Silver and ceria nanoparticles are both synthesized using the sol−gel method but with different reducing agents: silver nanoparticles use gum acacia, while ceria nanoparticles use dextrose. XRD measurement results on both nanoparticles confirmed the formation of nanoparticles and examined their crystal properties. Figure 1A is the diffractogram of AgNPs, which shows peaks at 2θ of 38.05°, 42.1°, 64.5°, and 77.05° corresponding to (111), (200), (220), and (311), respectively, of a face-centered cubic

https://doi.org/10.1021/acsomega.3c04575
ACS Omega 2023, 8, 39194−39202

Table 2. UV−vis Analysis of Carrageenan-Based Bionanocomposites[a]

treatment	T_{280}	T_{600}	transparency
BK-K	18.915 ± 1.675[b]	19.256 ± 1.103[b]	14.967 ± 1.856[b]
BK-AG1	4.908 ± 5.424[a]	10.352 ± 3.008[a]	12.462 ± 1.249[ab]
BK-CE0	0.044 ± 0.039[a]	14.584 ± 2.755[ab]	13.050 ± 0.675[ab]
BK-CE1	0.005 ± 0.001[a]	10.278 ± 4.016[a]	11.284 ± 3.451[ab]
BK-CE2	0.004[a]	9.516 ± 1.079[a]	9.257 ± 1.384[a]

[a]Values listed in the table are average ± standard deviation. Values in the same column followed by the same letter are not significantly different from each other ($p > 0.05$).

(fcc) silver crystal based on JCPDS 04-073.[30] Whereas, the formation of CeNPs is confirmed by X-ray diffraction analysis, which shows peaks at 2θ of 28.4° (111), 32.7° (200), 47.2° (220), 56.1° (311), 76.7° (331), and 77.3° (420) representing the crystal planes of the fcc crystal of CeO_2 (JCPDS 34-0394).

From XRD analysis, we obtained that the average crystallite size of ceria nanoparticles was smaller (3.54 nm) than silver nanoparticles (5.2 nm). The same results are also visible with the average size of nanoparticles analyzed by PSA, which shows that CeNPs are 42.69 nm in average size with a polydispersity index (PI) of 0.50, while AgNPs are 82.71 nm with a PI of 0.40. Morphological analysis of nanoparticles shown in Figures 1B and 2B shows that nanoparticles were formed. Figure 1B shows that the silver nanoparticles are spherical and have a size range of 5.7−18.9 nm, with some larger particles due to agglomeration. CeNPs were seen with a darker area (Figure 1D), and dextrose as a capping agent was seen as a brighter area surrounding the darker area. The TEM image also confirmed that formed CeNPs have smaller size than AgNPs; it shows that formed CeNPs have a size ranging from 1.4 to 10 nm with an average size of 4.075 nm with some agglomeration in several spots.

Incoroporation of Nanoparticles in a Bionanocomposite Polymer Film. The surface morphology of bionanocomposites can be seen in Figure 2; the morphology of carrageenan bionanocomposites appears to differ in topography and the presence of "ghosts" that appear to be protruding structures. "Ghosts" are starch particles that can persist as hydrated swollen starch due to incomplete gelatinization.[31] Figure 2B also shows that bionanocomposites without nanoparticles have a smoother surface than those with nanoparticles. The difference in the surface structure is due to the homogeneity of surface morphology after nanoparticle addition.[32] Moreover, cerium bionanocomposites exhibit a

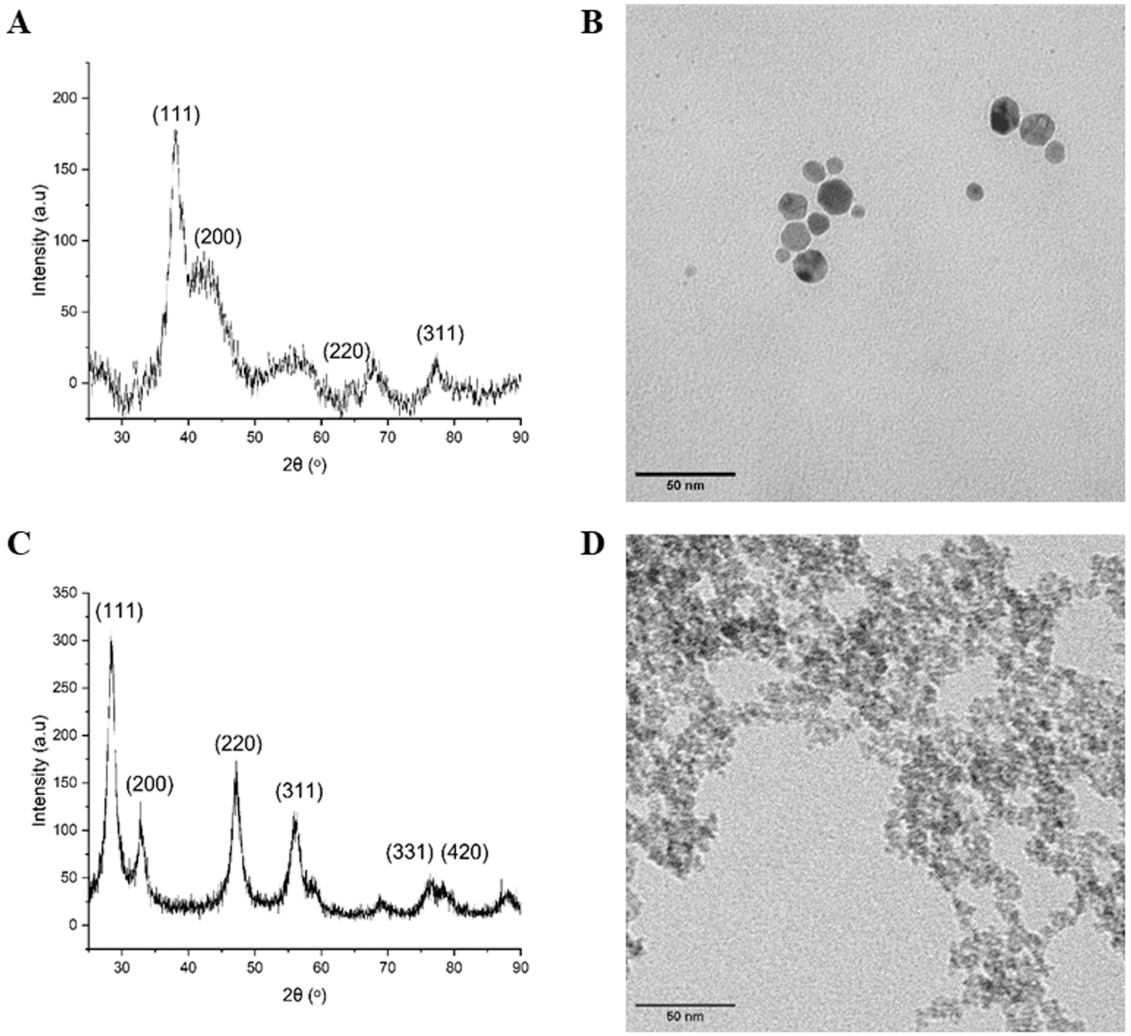

Figure 1. Characterization of silver nanoparticles. (A) XRD diffractogram of AgNPs, (B) TEM image of AgNPs, (C) XRD diffractogram of CeNPs, and (D) TEM image of CeNPs.

https://doi.org/10.1021/acsomega.3c04575
ACS Omega 2023, 8, 39194−39202

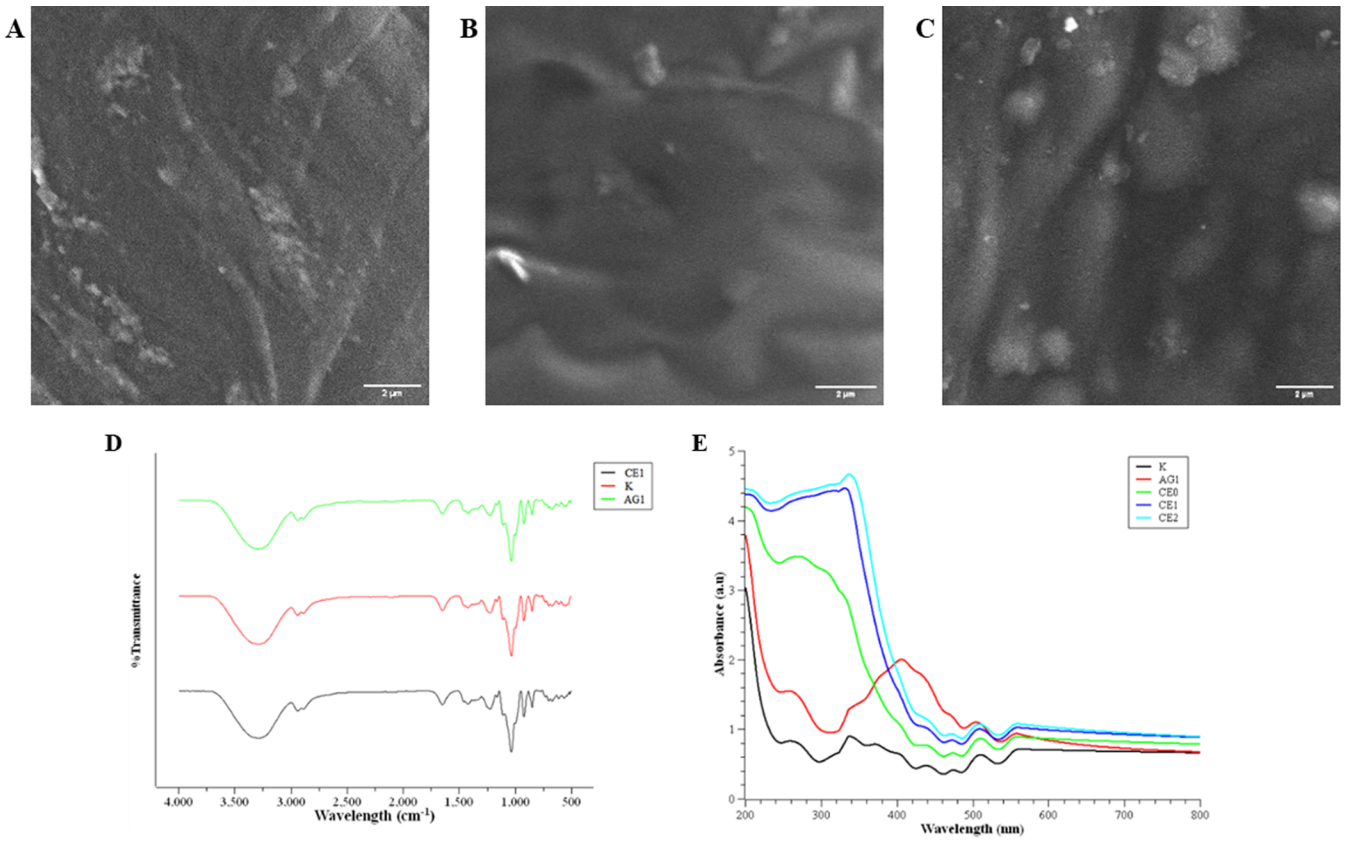

Figure 2. SEM image of carrageenan-based bionanocomposites. (A) BK-CE1, (B) BK-K, and (C) BK-AG1. (D) FTIR spectrum of carrageenan-based bionanocomposites and (E) UV−vis spectra of carrageenan-based bionanocomposites.

smoother surface than silver bionanocomposites (Figure 2A). The difference in nanoparticle size can be one factor causing the phenomenon described, as it is known that the larger the molecular size, the lower the ability of nanoparticles to penetrate the polymer structure.[33]

The FTIR spectra of carrageenan bionanocomposites films are shown in Figure 2D. All films exhibit characteristic peaks of carrageenan in 3200−3600 cm^{-1} due to the vibration of −OH groups.[34] The peak at 2800−2900 cm^{-1} results from the vibration of C−H bonds in the alkane groups of the carrageenan polymer.[22] An amide peak was seen at 1664 cm^{-1}, which was prevalent throughout the nanocomposite film spectrum.[34] The peak observed at 1218 cm^{-1} was the peak for the sulfated ester group of carrageenan.[35] Other carrageenan characteristics were observed through the 920 and 844 cm^{-1} peaks, representing the 3,6-anhydrous-D-galactose and galactose-4-sulfate bonds, respectively.[22] Peaks at 511 cm^{-1} also appear in all bionanocomposites samples and represent the Si−O bending of MMT.[36] The FTIR spectrum does not show any peaks from Ag metal as the Ag metal peak is outside the spectrum of analysis at a range around 386 cm^{-1}.[37] In general, as shown in Figure 2D, there is no significant change in the functional groups of the nanocomposites, which indicates no change in chemical bonding in the bionanocomposite film with the addition of nanoparticles.

Functional Properties of a Bionanocomposite Polymer Film as Food Packaging. Food packaging materials have an important role in providing protection for food products from environmental, chemical, and physical damage. Good packaging can protect food from physical damage and provide barriers to moisture, oxygen, carbon dioxide, and other gases, as well as flavors and aromas. Food products are also sensitive to UV light since they can induce food nutritional content degradation, such as protein, vitamin B, and other antioxidant molecules.[38,41,46] Protection against light, particularly UV light, is also required for food packaging. In addition to physical and chemical protection, protection against microbiological hazards is also an important role of food packaging. As food safety needs to be guaranteed and maintained, it is closely related to food contamination and damage due to microbial activity in packaged food.

Spectrophotometry analysis results are presented in Figure 2E. The result shows that silver and cerium bionanocomposites exhibit better UV barrier protection than without nanoparticle addition. The absorption peak of BK-AG1 is seen at 410 nm due to silver nanoparticles with a plasmonic effect at wavelengths of 410−480 nm.[22,39] While in cerium bionanocomposites, high absorbance values above 2 au (1% maximum transmittance) were observed for wavelengths below 350 nm, and the absorption peak was observed around the wavelength of 340 nm. Moreover, the absorbance values increased by the increase in cerium nanoparticle concentration (Figure 2E). These UV−vis results show that cerium bionanocomposites exhibit an excellent UV barrier property, consistent with Dao et al.'s findings in 2011, which observed that an epoxy nanocomposite with the addition of cerium oxide nanoparticles can absorb more than 90% of UV light.[40] A significant decrease in transmission is also seen due to the presence of nanoparticles (Table 2), and it plays a role in preventing light from entering the polymer matrix. However, the addition of nanoparticles also reduces the transparency of the film.

https://doi.org/10.1021/acsomega.3c04575
ACS Omega 2023, 8, 39194−39202

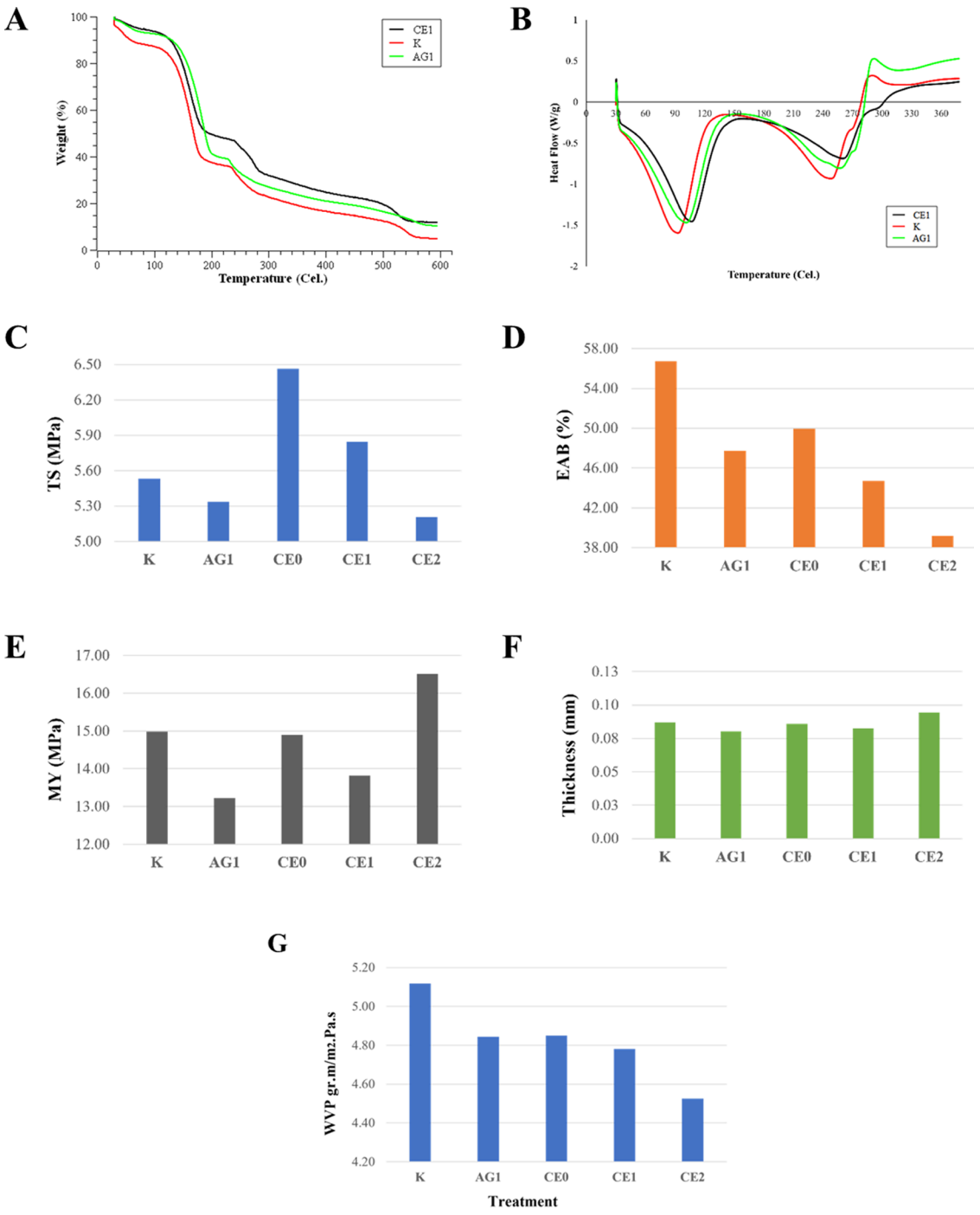

Figure 3. (A) Thermogravimetric analysis, (B) DSC analysis, (C) tensile strength, (D) elongation, (E) Young's modulus, (F) thickness, and (G) WVP of carrageenan-based bionanocomposites.

Thermal decomposition of carrageenan bionanocomposites is found to occur in several stages (Figure 3A). The first stage is observed at around 100 °C, which is found to be due to the desorption of water molecules in the polymer. The second stage of decomposition occurred at around 200 °C, which is explained by volatilization of the glycerol plasticizer or degradation of low-molecular-weight molecules. The third stage of decomposition is polysaccharide decomposition, which forms a polymer matrix, usually occurring at a temperature above 250 °C.[22,41] Finally, the last stage of decomposition above 500 °C occurs due to the water hydrogen bond structure in the montmorillonite interlayer.[42]

Thermal analysis results exhibited improved thermal stability of bionanocomposites incorporated with nanoparticles, as is seen from the shift of endothermic and exothermic peaks at the DSC results (Figure 3B), where the addition of nanoparticles shifted the peaks to higher values. DSC results also show that the cerium bionanocomposites exhibit better thermal stability than silver bionanocomposites, where endothermic peaks for BC-CE1 are at higher temperatures than that of BC-AG1. Meanwhile, the exothermic peak of BC-CE1 cannot be observed clearly; that is most likely due to the overlap between the broad second endothermic curve and the exothermic curve of BC-CE1. Furthermore, TGA results also show that the

https://doi.org/10.1021/acsomega.3c04575
ACS Omega 2023, 8, 39194−39202

Table 3. WVP Analysis of Carrageenan-Based Bionanocomposites[a]

treatment	WVP ($\times 10^{-13}$)	WVTR (g/m·s/day)
BC-K	5.12 ± 0.30[a]	31.41 ± 2.97[a]
BC-AG1	4.84 ± 1.38[a]	30.87 ± 8.24[a]
BC-CE0	4.85 ± 1.86[a]	29.27 ± 7.99[a]
BC-CE1	4.78 ± 0.97[a]	30.50 ± 4.12[a]
BC-CE2	4.53 ± 1.13[a]	25.12 ± 3.58[a]

[a]Values listed in the table are average ± standard deviation. Values in the same column followed by the same letter are not significantly different from each other ($p > 0.05$).

Table 4. Antibacterial Activity of Carrageenan-Based Bionanocomposites[a]

	inhibition zone (mm)	
treatment	*Escherichia coli*	*Bacillus cereus*
BC-K	5.64 ± 2.54[b]	2.68 ± 1.13[ab]
BC-AG1	6.02 ± 1.72[b]	6.83 ± 0.94[c]
BC-CE0	7.46 ± 1.46[b]	4.36 ± 0.92[bc]
BC-CE1	7.64 ± 2.29[b]	4.58 ± 1.68[bc]
BC-CE2	7.87 ± 2.48[b]	4.77 ± 1.76[bc]
aquadest	0[a]	0[a]
penicilin	19.07 ± 4.68[c]	11.03 ± 3.62[d]

[a]Values listed in the table are average ± standard deviation. Values in the same column followed by the same letter are not significantly different from each other ($p > 0.05$).

residual values of BC-K, BC-AG1, and BC-CE1, respectively, are 4.82%, 10.35%, and 11.77%; this result is also evidence that shows that nanoparticle addition could increase the thermal stability of bionanocomposites where CeNPs' addition give the best thermal stability. Thus, the results show that incorporating nanoparticles can improve the crystallinity of polymers, as evidenced by the differences in residuals after thermal analysis.[44,45]

More finding on thermal analysis is that carrageenan bionanocomposites (Figure 3B) do not show any feature indicating the composites' glass transition temperature, likely due to the decrease in transition glass temperature (T_g). The decrease in T_g is due to the decrease in intermolecular forces of the polymer caused by the addition of water and a plasticizer during the synthesis of composites. This decrease in T_g also correlates with the decrease in the EAB value and an increase in TS in mechanical properties, which is also shown in this research's results (Figure 3C,3D).[43]

The addition of nanoparticles in the bionanocomposite also causes a decrease in % elongation of the film (Figure 3D), which leads to a decrease in film flexibility. The addition of nanoparticles causes a decrease in water absorption into the film, altering molecular interactions and reducing the ability of water to act as a mobility enhancer, thus affecting film flexibility.[43] The integration of nanoparticles also affects the tensile strength of bionanocomposites (Figure 3C). Cerium bionanocomposites show an increase in tensile strength (Figure 3C) due to the interaction of nanoparticles as fillers with the polymer matrix, resulting in the expansion of the contact area during stress, which becomes influential in film strength.[22,49] Unlike some previous studies,[22] adding silver nanoparticles to bionanocomposites decreased the TS value in this study. Low dispersion and agglomeration may explain the decrease in the TS value, causing stress concentration points in the composite and leading to crack initiation.[49]

A decrease in WVP is seen in nanocomposites after adding nanoparticles (Figure 3G), which is aligned with the study by Rhim and Wang in 2020 that observed a decrease in WVP of a chitosan-based nanocomposite film after the addition of MMT and silver nanoparticles. The decrease in permeability corresponds to the addition of nanoparticles that can obstruct the path of water vapor, affecting the diffusion rate of water molecules and increasing the film's barrier properties. Moreover, a trend of decreasing WVP is also shown in Figure 3G, as the concentration of ceria nanoparticles increases, due to the increasing nanofiller volume, which alters the permeability of nanocomposites. Three main factors affect the permeability of nanocomposites: (1) the volume fraction of nanofillers or nanoplatelets, (2) the orientation of nanoplatelets toward the diffusion direction, and (3) the aspect ratio of nanoplatelets.[48] However, the permeability of a nanocomposite film exhibits no significant difference compared to carrageenan-based films ($p > 0.05$), as shown in Table 3. This may occur due to a filler dispersion problem, which can happen due to the agglomeration of nanoparticles. The filler dispersion problem inhibits the uniform distribution of nanoparticles in the polymer matrix, which alters the permeability and mechanical properties of the polymer matrix.[47]

The antimicrobial activity of a carrageenan-based bionanocomposite film was tested by an agar diffusion method against two common foodborne pathogens, *E. coli* and *B.cereus*. The results of the antimicrobial activity were determined by the film samples' inhibition zone diameter (DI). As expected, the results showed that all bionanocomposites had antimicrobial activity for Gram-positive and Gram-negative bacteria (Table 4). The carrageenan bionanocomposite has an inhibition zone (DI) of Gram-negative bacteria larger than Gram-positive bacteria. This result is in line with the results of a study by Rhim et al. in 2014 that also showed the antimicrobial activity of carrageenan-mineral clay nanocomposites, which is due to the existence of alkylamine or quaternary ammonium groups that can bind phospholipids and proteins disrupting the lipid bilayer of microbial membranes, leading to lysis of the microbial cell.[39]

Furthermore, Table 4 shows an increased inhibition zone after the addition of silver and cerium nanoparticles. A silver bionanocomposite tends to inhibit the growth of Gram-positive bacteria more than Gram-negative bacteria, which may happen due to the higher affinity of lipopolysaccharides in Gram-negative bacteria compared to Gram-positive bacteria. These lipopolysaccharides then trap Ag^+ ions and hinder the antimicrobial performance of AgNPs.[50] Several hypotheses have been explained to describe the antimicrobial activity of silver nanoparticles, including the production of reactive oxygen species (ROS), the release of Ag^+ ions that causes denaturation of proteins' sulfhydryl bonds, and the attachment of bacteria to AgNPs that can cause damage to bacteria.[51] In contrast with silver bionanocomposites, cerium bionanocomposites tend to inhibit Gram-negative bacteria. The difference in the antimicrobial effect is related to the structure and compactness of Gram-positive and Gram-negative bacteria cell walls. Gram-positive bacteria have thicker cell walls, making them more resistant than Gram-negative bacteria.[27]

https://doi.org/10.1021/acsomega.3c04575
ACS Omega 2023, 8, 39194−39202

CONCLUSIONS

In this study, incorporating silver and ceria nanoparticles into carrageenan-based bionanocomposites has successfully improved bionanocomposite characteristics, such as mechanical strength, permeability, thermal stability, UV light resistance, and antimicrobial activity. The antimicrobial activity of carrageenan-based bionanocomposites is visible against Gram-positive and Gram-negative bacteria. However, the inhibition of bacteria growth tendencies differed depending on the added nanoparticles. Silver bionanocomposites exhibited better antimicrobial activity against Gram-positive bacteria, while ceria bionanocomposites exhibited better antimicrobial activity against Gram-negative bacteria. Furthermore, adding ceria nanoparticles resulted in better UV barrier properties with decreased transparency. The best mechanical properties were achieved for CeNPs addition of 0.5%. Nanoparticle addition enhances the composite film barrier properties by lowering the WVP and improving thermal stability. These results suggest that carrageenan-based bionanocomposites have a high potential as active food packaging applications to secure food safety and prolong the shelf life of packaged foods.

AUTHOR INFORMATION

Corresponding Author

Damar R. Adhika − *Advanced Functional Materials Research Group, Faculty of Industrial Technology and Research Center for Nanosciences and Nanotechnology, Gd. Center for Advance Sciences, Institut Teknologi Bandung, 40132 Bandung, West Java, Indonesia;* orcid.org/0000-0003-0961-5039; Email: damar@itb.ac.id

Authors

Gita Genecya − *Magister of Nanotechnology, Graduate School, Institut Teknologi Bandung, 40132 Bandung, West Java, Indonesia*

Widayani Sutrisno − *Nuclear Physics and Biophysics Research Group, Faculty of Mathematics and Natural Sciences, Institut Teknologi Bandung, 40132 Bandung, West Java, Indonesia*

Triati D. K. Wungu − *Nuclear Physics and Biophysics Research Group, Faculty of Mathematics and Natural Sciences and Research Center for Nanosciences and Nanotechnology, Gd. Center for Advance Sciences, Institut Teknologi Bandung, 40132 Bandung, West Java, Indonesia*

Complete contact information is available at: https://pubs.acs.org/10.1021/acsomega.3c04575

Notes

The authors declare no competing financial interest.

ACKNOWLEDGMENTS

The authors express gratitude to Indonesian Government Kemdikbudristek Research Grant PDUPT 2022 with contract number 187/E5/PG.02.00.PT/2022.

REFERENCES

(1) Alabi, O.; Ologbonjaye, K.; Awosolu, O.; Alalade, O. E. Public and Environmental Health Effects of Plastic Wastes Disposal: A Review. *J. Toxicol. Risk Assess* **2019**, *5*, 1−13, DOI: 10.23937/2572-4061.1510021.

(2) Shlush, E.; Davidovich-Pinhas, M. Bioplastics for food packaging. *Trends Food Sci. Technol.* **2022**, *125*, 66−80.

(3) Sudhakar, M. P.; Venkatnarayanan, S.; Dharani, G. Fabrication and characterization of bio-nanocomposite films using κ-Carrageenan and Kappaphycus alvarezii seaweed for multiple industrial applications. *Int. J. Biol. Macromol.* **2022**, *219*, 138−149.

(4) Aga, M. B.; Dar, A. H.; Nayik, G. A.; et al. Recent insights into carrageenan-based bio-nanocomposite polymers in food applications: A review. *Int. J. Biol. Macromol.* **2021**, *192*, 197−209.

(5) *Bioplastics for Sustainable Development*; Kuddus, M.; Roohi, Eds.; Springer Singapore: Singapore, 2021.

(6) Roy, S.; Van Hai, L.; Kim, H. C.; Zhai, L.; Kim, J. Preparation and characterization of synthetic melanin-like nanoparticles reinforced chitosan nanocomposite films. *Carbohydr. Polym.* **2020**, *231*, No. 115729.

(7) Álvarez-Chávez, C. R.; Edwards, S.; Moure-Eraso, R.; Geiser, K. Sustainability of bio-based plastics: general comparative analysis and recommendations for improvement. *J. Clean. Prod.* **2012**, *23* (1), 47−56.

(8) Song, J.; Kay, M.; Coles, R. Bioplastics. In *Food and Beverage Packaging Technology*, 2nd ed.; Wiley, 2011; pp 295−319.

(9) Anugrahwidya, R.; Armynah, B.; Tahir, D. Bioplastics Starch-Based with Additional Fiber and Nanoparticle: Characteristics and Biodegradation Performance: A Review. *J. Polym. Environ.* **2021**, *29* (11), 3459−3476.

(10) Karan, H.; Funk, C.; Grabert, M.; Oey, M.; Hankamer, B. Green Bioplastics as Part of a Circular Bioeconomy. *Trends Plant Sci.* **2019**, *24* (3), 237−249.

(11) Porta, R.; Sabbah, M.; Di Pierro, P. Biopolymers as Food Packaging Materials. *Int. J. Mol. Sci.* **2020**, *21*, 4942.

(12) Dang, B.-T.; Bui, X. T.; Tran, D. P.; et al. Current application of algae derivatives for Bioplastic production: A review. *Bioresour. Technol.* **2022**, *347*, No. 126698.

(13) Rasmussen, R. S.; Morrissey, M. T. Marine Biotechnology for Production of Food Ingredients. In *Advances in Food and Nutrition Research*; Elsevier, 2007; pp 237−292.

(14) Shojaee-Aliabadi, S.; Mohammadifar, M. A.; Hosseini, H.; et al. Characterization of nanobiocomposite kappa-carrageenan film with Zataria multiflora essential oil and nanoclay. *Int. J. Biol. Macromol.* **2014**, *69*, 282−289.

(15) De Ruiter, G. A.; Rudolph, B. Carrageenan biotechnology. *Trends Food Sci. Technol.* **1997**, *8* (12), 389−395.

(16) Nguyen, L. N. Seaweed Carrageenans: Productions and Applications. In *Biomass, Biofuels, and Biochemicals*; Ngo, H.; Guo, W.; Pandey, A.; Chang, J.-S.; Lee, D.-J., Eds.; Elsevier, 2022, Chapter 4, pp 67−80.

(17) Sedayu, B. B.; Cran, M. J.; Bigger, S. W. A Review of Property Enhancement Techniques for Carrageenan-based Films and Coatings. *Carbohydr. Polym.* **2019**, *216*, 287−302.

(18) Berk, Z. Food Packaging. In *Food Process Engineering and Technology*; Elsevier, 2013; pp 621−636.

(19) Bhat, A. H.; Khan, I.; Amil Usmani, M.; Rather, J. A. Bioplastics and Bionanocomposites Based on Nanoclays and Other Nanofillers. In *Nanoclay Reinforced Polymer Composites*; Jawaid, M.; el, A.; Qaiss, K.; Bouhfid, R., Eds.; Engineering Materials; Springer: Singapore, 2016; pp 115−139.

(20) Kanmani, P.; Rhim, J.-W. Physical, mechanical and antimicrobial properties of gelatin based active nanocomposite films containing AgNPs and nanoclay. *Food Hydrocolloids* **2014**, *35*, 644−652.

(21) Uddin, F. Montmorillonite: An Introduction to Properties and Utilization. In *Current Topics in the Utilization of Clay in Industrial and Medical Applications*; IntechOpen, 2018.

(22) Rhim, J. W.; Wang, L. F. Preparation and characterization of carrageenan-based nanocomposite films reinforced with clay mineral and silver nanoparticles. *Appl. Clay Sci.* **2014**, *97-98*, 97−98.

(23) Llorens, A.; Lloret, E.; Picouet, P. A.; Trbojevich, R.; Fernandez, A. Metallic-based micro and nanocomposites in food contact materials and active food packaging. *Trends Food Sci. Technol.* **2012**, *24* (1), 19−29.

(24) Malhotra, B. D.; Ali, M. A. Nanomaterials in Biosensors: Fundamentals and Applications. In *Nanomaterials for Biosensors*;

Malhotra, B. D.; Ali, M. A., Eds.; Micro and Nano Technologies; William Andrew Publishing, 2018; Chapter 1, pp 1−74.
(25) Hoseinnejad, M.; Jafari, S.; Katouzian, I. Inorganic and metal nanoparticles and their antimicrobial activity in food packaging applications. *Crit. Rev. Microbiol.* **2017**, *44*, 1−21.
(26) Abass Sofi, M.; Sunitha, S.; Ashaq Sofi, M.; Khadheer Pasha, S. K.; Choi, D. An overview of antimicrobial and anticancer potential of silver nanoparticles. *J. King Saud Univ. Sci.* **2022**, *34* (2), No. 101791.
(27) Nadeem, M. Green Synthesis of Cerium Oxide Nanoparticles (CeO_2 NPs) and Their Antimicrobial Applications: A Review. *Int. J. Nanomed.* **2020**, *15*, 5951−5961.
(28) Asati, A.; Santra, S.; Kaittanis, C.; Perez, J. M. Surface-Charge-Dependent Cell Localization and Cytotoxicity of Cerium Oxide Nanoparticles. *ACS Nano* **2010**, *4* (9), 5321−5331.
(29) Dong, C.; Zhang, X.; Cai, H.; Cao, C. Facile and one-step synthesis of monodisperse silver nanoparticles using gum acacia in aqueous solution. *J. Mol. Liq.* **2014**, *196*, 135−141.
(30) Gurunathan, S.; Jeong, J.-K.; Han, J.; Zhang, X.-F.; Park, J.; Kim, J.-H. Multidimensional effects of biologically synthesized silver nanoparticles in Helicobacter pylori, Helicobacter felis, and human lung (L132) and lung carcinoma A549 cells. *Nanoscale Res. Lett.* **2015**, *10*, No. 35, DOI: 10.1186/s11671-015-0747-0.
(31) Hernández-Jaimes, C.; Meraz, M.; Lara, V. H.; Blanco, G.; Buendía-González, L. Acid hydrolysis of composites based on corn starch and trimethylene glycol as plasticizer. *Rev. Mex. Ing. Quim.* **2017**, *16*, 169−178.
(32) Amin, M. R.; Chowdhury, M. A.; Kowser, M. A. Characterization and performance analysis of composite bioplastics synthesized using titanium dioxide nanoparticles with corn starch. *Heliyon* **2019**, *5* (8), No. e02009.
(33) Davoodi, M. N.; Milani, J. M.; Farahmandfar, R. Preparation and characterization of a novel biodegradable film based on sulfated polysaccharide extracted from seaweed *Ulva intestinalis*. *Food Sci. Nutr.* **2021**, *9* (8), 4108−4116.
(34) Hezaveh, H.; Muhamad, I. I. Modification and swelling kinetic study of kappa-carrageenan-based hydrogel for controlled release study. *J. Taiwan Inst. Chem. Eng.* **2013**, *44* (2), 182−191.
(35) Distantina, S.; Rochmadi, R.; Fahrurrozi, M.; Wiratni, W. Synthesis of Hydrogel Film Based on Carrageenan Extracted from Kappaphycus alvarezii. *Mod. Appl. Sci.* **2013**, *7* (8), 22.
(36) Sanusi, O. M.; Benelfellah, A.; Papadopoulos, L.; Terzoupoulu, Z.; Bikiaris, D. N.; Hocine, N. A. Properties of poly(lactic acid)/montmorillonite/carbon nanotubes nanocomposites: determination of percolation threshold. *J. Mater. Sci.* **2021**, *56*, 16887−16901, DOI: 10.1007/s10853-021-06378-z.
(37) Pawar, O.; Deshpande, N.; Gadale -Dagade, S.; Waghmode, S.; Nigam, P.; Joshi, N. Green synthesis of silver nanoparticles from purple acid phosphatase apoenzyme isolated from a new source Limonia acidissima. *J. Exp. Nanosci.* **2015**, *11*, 28−37, DOI: 10.1080/17458080.2015.1025300.
(38) Duncan, S. E.; Hannah, S. Light-protective packaging materials for foods and beverages. In *Emerging Food Packaging Technologies*; Elsevier, 2012; pp 303−322 and.
(39) Kim, Y. H.; Bang, Y.-J.; Yoon, K. S.; Priyadarshi, R.; Rhim, J.-W. Pine Needle (Pinus densiflora) Extract-Mediated Synthesis of Silver Nanoparticles and the Preparation of Carrageenan-Based Antimicrobial Packaging Films. *J. Nanomater.* **2022**, *2022*, 1−15.
(40) Dao, N. N.; Luu, M. D.; Nguyen, Q. K.; Kim, B. S. UV absorption by cerium oxide nanoparticles/epoxy composite thin films. *Adv. Nat. Sci. Nanosci. Nanotechnol.* **2011**, *2* (4), No. 045013.
(41) Heidari, M.; Khomeiri, M.; Yousefi, H.; Rafieian, M.; Kashiri, M. Chitin nanofiber-based nanocomposites containing biodegradable polymers for food packaging applications. *J. Consum. Prot. Food Saf.* **2021**, *16* (3), 237−246.
(42) Qin, D.; Chang, S.; Qiao, M.; Yuan, X.; Liu, W.; Liu, G. An evaluation of the adsorption dynamics of phosphate ions ontoFe(II)-montmorillonites. *Turk. J. Chem.* **2019**, *43* (1), 50−62.
(43) Ili Balqis, A. M.; Nor Khaizura, M. A. R.; Russly, A. R.; Nur Hanani, Z. A. Effects of plasticizers on the physicochemical properties of kappa-carrageenan films extracted from Eucheuma cottonii. *Int. J. Biol. Macromol.* **2017**, *103*, 721−732.
(44) El Fray, M.; Strzalkowska, D.; Mandoli, C.; Pagliari, F.; Di Nardo, P.; Traversa, E. Influence of ceria nanoparticles on chemical structure and properties of segmented polyesters. *Mater. Sci. Eng., C* **2015**, *53*, 15−22.
(45) Watase, M.; Nishinari, K. Rheology, DSC and Volume or Weight Change Induced by Immersion in Solvents for Agarose and Kappa-Carrageenan Gels. *Polym. J.* **1986**, *18* (12), 1017.
(46) Sudhakar, M. P.; Magesh Peter, D.; Dharani, G. Studies on the development and characterization of Bioplastic film from the red seaweed (Kappaphycus alvarezii). *Environ. Sci. Pollut. Res.* **2021**, *28* (26), 33899−33913.
(47) Sarfraz, J.; Gulin-Sarfraz, T.; Nilsen-Nygaard, J.; Pettersen, M. K. Nanocomposites for Food Packaging Applications: An Overview. *Nanomaterials* **2021**, *11* (1), 10.
(48) Choudalakis, G.; Gotsis, A. D. Permeability of polymer/clay nanocomposites: A review. *Eur. Polym. J.* **2009**, *45* (4), 967−984.
(49) Boey, J. Y.; Lee, C. K.; Tay, G. S. Factors Affecting Mechanical Properties of Reinforced Bioplastics: A Review. *Polymers* **2022**, *14* (18), 3737.
(50) Lara, H.; Ayala-Nunez, V.; Ixtepan Turrent, L.; Rodríguez-Padilla, C. Bactericidal effect of AgNPs against multidrug-resistant bacteria. *World J. Microbiol. Biotechnol.* **2010**, *26*, 615−621.
(51) Urnukhsaikhan, E.; Bold, B.-E.; Gunbileg, A.; Sukhbaatar, N.; Mishig-Ochir, T. Antibacterial activity and characteristics of silver nanoparticles biosynthesized from Carduus crispus. *Sci. Rep.* **2021**, *11* (1), No. 21047, DOI: 10.1038/s41598-021-00520-2.

https://doi.org/10.1021/acsomega.3c04575
ACS Omega 2023, 8, 39194−39202